

Analysis of the Multimodulus Blind Equalization Algorithm in QAM Communication Systems

Jenq-Tay Yuan, *Senior Member, IEEE*, and Kun-Da Tsai

Abstract—The constant modulus algorithm (CMA) for blind equalization requires a separate carrier-recovery system for phase recovery. This letter mathematically analyzes a modified CMA, called the multimodulus algorithm (MMA), which may perform joint blind equalization and carrier recovery without the need for a separate carrier-recovery system for quadrature amplitude modulation signal constellations. The analyses focus on five aspects of the MMA: 1) derivation of the general formulation of the MMA cost function; 2) stationary points of the MMA; 3) desired global minima of the MMA; 4) unstable equilibria (saddle points) of the MMA; and 5) analytic verification of a discrete-time first-order phase-locked loop hidden inside the MMA, which is absent from the conventional CMA. Analysis results indicate that the MMA alone may be able to remove intersymbol interference and simultaneously correct the phase error, because it implicitly incorporates a phase-tracking loop, which automatically recovers carrier phase.

Index Terms—Blind equalization, carrier frequency offset (CFO), constant modulus algorithm (CMA), intersymbol interference (ISI), multimodulus algorithm (MMA), phase-locked loop (PLL), quadrature amplitude modulation (QAM).

I. INTRODUCTION

ADAPTIVE channel equalization without a training sequence is known as blind equalization [1]–[4]. A baseband model with a channel impulse response, channel input, additive white Gaussian noise (AWGN), and equalizer input are denoted by $c(n)$, $s(n)$, $w(n)$, and $u(n)$, respectively. The data symbols transmitted, $s(n)$, are assumed to consist of stationary independently and identically distributed (i.i.d.), real or complex non-Gaussian random variables. The equalizer input $u(n) = s(n) * c(n) + w(n)$ is then sent to a tap-delay-line blind equalizer with impulse response $f(n)$, intended to equalize the distortion caused by intersymbol interference (ISI) without a training signal. The output of the blind equalizer

$$\begin{aligned} y(n) &= u(n) * f(n) \\ &= s(n) * h(n) + w(n) * f(n) \\ &= \sum_i h(i) s(n-i) + \sum_i f(i) w(n-i) \end{aligned}$$

Paper approved by C.-L. Wang, the Editor for Modulation, Detection, and Equalization of the IEEE Communications Society. Manuscript received December 19, 2003; revised October 20, 2004 and January 12, 2005. This work was supported by the National Science Council, Taiwan, R.O.C., under Contract NSC 92-2213-E-030-009. This paper was presented in part at the 7th International Symposium on Signal Processing and Its Applications, Paris, France, July 2003.

J.-T. Yuan is with the Department of Electronic Engineering, Fu Jen Catholic University, Taipei 24205, Taiwan, R.O.C. (e-mail: yuan@ee.fju.edu.tw)

K.-D. Tsai is with the Department of Electronic Engineering, Fu Jen Catholic University, Taipei 24205, Taiwan, R.O.C. He is now with Lite-on Technology Corp., Taipei 115, Taiwan, R.O.C. (e-mail: isaac.tsai@liteon.com) Digital Object Identifier 10.1109/TCOMM.2005.855017

can be used to recover the transmitted data symbols $s(n)$, where $h(n) = c(n) * f(n)$ denotes the impulse response of the combined channel-equalizer system.

The constant modulus algorithm (CMA), whose cost function is $J_{\text{CMA}}(n) = E\{|y(n)|^2 - R_2\}^2$, where $R_2 = E\{|s(n)|^4\}/E\{|s(n)|^2\}$, is one of the most widely used blind equalization algorithms. Since the CMA cost function is invariant to a phase rotation in the constellation, consequently, the equalizer output signal constellation suffers from an arbitrary phase rotation. A rotator that can rotate the constellation back in the right position at the output of the equalizer is therefore needed in steady-state operation. Oh and Chin [5], and Yang *et al.* [6] proposed a modified CMA called the multimodulus algorithm (MMA), whose cost function is

$$\begin{aligned} J_{\text{MMA}}(n) &= J_R(n) + J_I(n) \\ &= E\{|y_R^2(n) - R_{2,R}\}^2 + E\{|y_I^2(n) - R_{2,I}\}^2 \end{aligned}$$

where $y_R(n)$ and $y_I(n)$ are the real and imaginary parts of the equalizer output, respectively; $R_{2,R}$ and $R_{2,I}$ are given by $R_{2,R} = E\{s_R^4(n)\}/E\{s_R^2(n)\}$ and $R_{2,I} = E\{s_I^4(n)\}/E\{s_I^2(n)\}$, in which $s_R(n)$ and $s_I(n)$ denote the real and imaginary parts of $s(n)$, respectively. Decomposing the cost function of MMA into the real and imaginary parts thus allows both the *modulus* and the *phase* of the equalizer output to be considered; therefore, joint *blind equalization* and *carrier-phase recovery* may be simultaneously accomplished, eliminating the need for a rotator to perform separate constellation-phase recovery in steady-state operation. The tap-weight vector of the MMA is updated according to

$$\mathbf{f}(n+1) = \mathbf{f}(n) - \mu \cdot e^*(n) \mathbf{u}(n) \quad (1)$$

where $e(n) = e_R(n) + je_I(n)$, in which $e_R(n) = y_R(n)(y_R^2(n) - R_{2,R})$ and $e_I(n) = y_I(n)(y_I^2(n) - R_{2,I})$.

This letter mathematically analyzes the MMA for quadrature amplitude modulation (QAM) signal constellations. The results of the analysis indicate that the MMA alone can remove ISI and simultaneously correct the phase error, because it implicitly incorporates a phase-tracking loop, which automatically recovers the carrier phase.

II. MMA COST FUNCTION FOR QAM SOURCE

The MMA cost function can be expressed as

$$\begin{aligned} J_{\text{MMA}}(n) &= J_R(n) + J_I(n) \\ &= E\{y_R^4(n)\} + E\{y_I^4(n)\} - 2R_{2,R} \cdot E\{y_R^2(n)\} \\ &\quad - 2 \cdot R_{2,I} \cdot E\{y_I^2(n)\} + R_{2,R}^2 + R_{2,I}^2. \end{aligned}$$

After some algebraic manipulation, the final expansion of the MMA cost function for a complex i.i.d. zero-mean QAM source, with each member of the symbol alphabet being

equiprobable and a complex baseband channel in additive white Gaussian zero-mean complex-valued rotationally invariant noise, can be expressed as

$$\begin{aligned}
J_{\text{MMA}}(n) &= \frac{1}{4} \Re \left\{ E \{ s^4(n) \} \sum_i h^4(i) \right\} + \frac{3}{4} \left(k_s \sigma_s^4 \sum_i |h(i)|^4 \right. \\
&\quad + 2\sigma_s^4 \sum_i \sum_{l \neq i} |h(i)|^2 |h(l)|^2 + k_w \sigma_w^4 \sum_j |f(j)|^4 \\
&\quad + 2\sigma_w^4 \sum_j \sum_{k \neq j} |f(j)|^2 |f(k)|^2 + 4\sigma_s^2 \sigma_w^2 \sum_i \sum_j |h(i)|^2 |f(j)|^2 \Big) \\
&\quad - \left(\left[\sigma_s^2 \sum_i |h(i)|^2 + \sigma_w^2 \sum_i |f(i)|^2 \right] [R_{2,I} + R_{2,R}] \right) \\
&\quad + R_{2,R}^2 + R_{2,I}^2 \tag{2}
\end{aligned}$$

where $\sigma_s^2 = E \{ |s(n)|^2 \}$, $\sigma_w^2 = E \{ |w(n)|^2 \}$, $k_s = E \{ |s(n)|^4 \} / \sigma_s^4$, and $k_w = E \{ |w(n)|^4 \} / \sigma_w^4$. The above final expansion can be compared with its CMA counterpart ([3, eq. (66)]). Evidently, the first term on the right-hand side of (2), $1/4 \Re [E \{ s^4(n) \} \sum_i h^4(i)]$, which contains the phase information of the blind equalizer output and is absent from the CMA cost function given by [3, eq. (66)], reveals the major difference between the CMA and the MMA. This phase information will later be shown to allow the MMA to recover a possible phase rotation of the equalizer output, resulting from a time-varying phase shift introduced by the channels.

III. ANALYSIS OF MMA

A. Stationary Points of the MMA

In noiseless QAM communication systems, (2) reduces to

$$\begin{aligned}
J_{\text{MMA}}(n) &= \frac{1}{4} E \{ s^4(n) \} \sum_i r^4(i) \cos 4\theta(i) \\
&\quad + \frac{3}{4} \left[k_s \sigma_s^4 \sum_i r^4(i) + 2\sigma_s^4 \sum_i \sum_{l \neq i} r^2(i) r^2(l) \right] \\
&\quad - 2\sigma_s^2 \frac{E \{ s_R^4(n) \}}{E \{ s_R^2(n) \}} \sum_i r^2(i) + 2 \left[\frac{E \{ s_R^4(n) \}}{E \{ s_R^2(n) \}} \right]^2 \tag{3}
\end{aligned}$$

where $h(k) = h_R(k) + jh_I(k) = r(k)e^{j\theta(k)}$ is the k th position of the combined channel-equalizer impulse response vector $\mathbf{h} = [\dots, h(-1), h(0), h(1), \dots]$ with $r(k) = \sqrt{h_R^2(k) + h_I^2(k)}$, $\theta(k) = \tan^{-1} h_I(k)/h_R(k)$.

For a prespecified $M \geq 1$ (during both transient and steady-state mode operations), the stationary points of the MMA can be found by setting the gradient of $J_{\text{MMA}}(n)$ in (3) to zero, such that

$$\nabla J_{\text{MMA}}(n) = \mathbf{r} \frac{\partial J_{\text{MMA}}(n)}{\partial r(k)} + \frac{\boldsymbol{\theta}}{r(k)} \frac{\partial J_{\text{MMA}}(n)}{\partial \theta(k)} = 0$$

yielding

$$\begin{aligned}
E \{ s^4(n) \} r^3(k) \cos 4\theta(k) + 3k_s \sigma_s^4 r^3(k) + 6\sigma_s^4 r(k) \\
\times \sum_{l \neq k} r^2(l) - 4 \frac{E \{ s_R^4(n) \}}{E \{ s_R^2(n) \}} \sigma_s^2 r(k) = 0 \tag{4}
\end{aligned}$$

$$E \{ s^4(n) \} r^3(k) [-\sin 4\theta(k)] = 0 \tag{5}$$

where \mathbf{r} and $\boldsymbol{\theta}$ are unit vectors in the $r(k)$ and $\theta(k)$ directions, respectively. Notably, (5) plays a role similar to that of a first-order phase-locked loop (PLL), and together with (4), the MMA may simultaneously remove ISI and correct the phase error, as will become apparent later. Since $E \{ s^4(n) \} \neq 0$ and $r^3(k) > 0$, (5) yields $\sin 4\theta(k) = 0$ or $\theta(k) = 0, \pi/4, \pi/2, 3\pi/4, \pi, 5\pi/4, 3\pi/2, 7\pi/4$. Equation (5) is crucial, as it restricts $\theta(k)$ to only eight different values. Equation (4) yields one result when $\theta(k) \in \{0, \pi/2, \pi, 3\pi/2\}$ (such that $\cos 4\theta(k) = 1$), and another when $\theta(k) \in \{\pi/4, 3\pi/4, 5\pi/4, 7\pi/4\}$ (such that $\cos 4\theta(k) = -1$). Therefore, all of the possible equilibria of the MMA can be grouped into two categories, according to the values of $\cos 4\theta(k)$. A general form for all possible stationary points of the MMA is now derived for both transient and steady-state mode operations.

Substituting $\theta(k) \in \{0, \pi/2, \pi, 3\pi/2\}$ into (4) yields

$$\begin{aligned}
[E \{ s^4(n) \} + 3k_s \sigma_s^4] r_+^3(k) \\
+ \left[6\sigma_s^4 \sum_{i \neq k} r_+^2(i) - 4\sigma_s^2 \frac{E \{ s_R^4(n) \}}{E \{ s_R^2(n) \}} \right] r_+(k) = 0, \\
k = 1, \dots, M. \tag{6}
\end{aligned}$$

Substituting $\theta(k) \in \{\pi/4, 3\pi/4, 5\pi/4, 7\pi/4\}$ into (4) yields

$$\begin{aligned}
[-E \{ s^4(n) \} + 3k_s \sigma_s^4] r_-^3(k) \\
+ \left[6\sigma_s^4 \sum_{i \neq k} r_-^2(i) - 4\sigma_s^2 \frac{E \{ s_R^4(n) \}}{E \{ s_R^2(n) \}} \right] r_-(k) = 0, \\
k = 1, \dots, M. \tag{7}
\end{aligned}$$

Clearly, (6) and (7) give $r_+^2(1) = r_+^2(2) = \dots = r_+^2(M)$ and $r_-^2(1) = r_-^2(2) = \dots = r_-^2(M)$, respectively. Consequently, (6) and (7), given $k = M$, suffice to determine both $r_+^2(M)$ and $r_-^2(M)$

$$\begin{aligned}
[E \{ s^4(n) \} + 3k_s \sigma_s^4] r_+^3(M) \\
+ \left[6\sigma_s^4 \sum_{i \neq M} r_+^2(i) - 4\sigma_s^2 \frac{E \{ s_R^4(n) \}}{E \{ s_R^2(n) \}} \right] r_+(M) = 0 \tag{8}
\end{aligned}$$

$$\begin{aligned}
[-E \{ s^4(n) \} + 3k_s \sigma_s^4] r_-^3(M) \\
+ \left[6\sigma_s^4 \sum_{i \neq M} r_-^2(i) - 4\sigma_s^2 \frac{E \{ s_R^4(n) \}}{E \{ s_R^2(n) \}} \right] r_-(M) = 0. \tag{9}
\end{aligned}$$

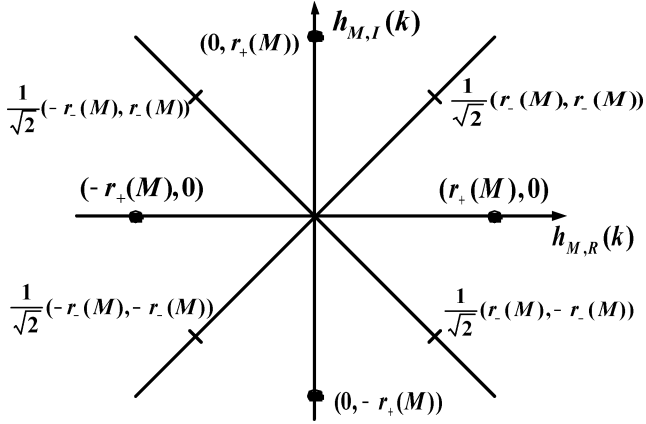


Fig. 1. Locations of all possible stationary points of the MMA for each $h_M(k)$, where $h_{M,R}(k)$ and $h_{M,I}(k)$ denote the real and imaginary parts of $h_M(k)$.

Using $E[s^4(n)] = 2E[s_R^4(n)] - 6E^2[s_R^2(n)]$, $k_s\sigma_s^4 = 2E[s_R^4(n)] + 2E^2[s_R^2(n)]$, and $\sigma_s^4 = 4E^2[s_R^2(n)]$, yields

$$r_+^2(M) = \frac{E\{s_R^4(n)\}}{E\{s_R^4(n)\} + [3(M-1)]E^2\{s_R^2(n)\}}$$

and

$$r_-^2(M) = \frac{2E\{s_R^4(n)\}}{E\{s_R^4(n)\} + [3(2M-1)]E^2\{s_R^2(n)\}}$$

which are directly solved by using (8) and (9), respectively. The following general form for all possible stationary points of the MMA can thus be derived:

$$|h_M(k)|^2 = \left[r_+^2(M) \sum_{i \in I_M \text{ and } \theta(k) \in \{0, \pi/2, \pi, 3\pi/2\}} \delta(k-i) \right] + \left[r_-^2(M) \sum_{i \in I_M \text{ and } \theta(k) \in \{\pi/4, 3\pi/4, 5\pi/4, 7\pi/4\}} \delta(k-i) \right] \quad (10)$$

where I_M is any set of M integers and $M = 1, 2, 3, \dots$ is the number of nonzero components of the set of stationary points $\mathbf{h}_M = [\dots, h_M(-1), h_M(0), h_M(1), \dots]^T$. Fig. 1 depicts the locations of all possible stationary points of the MMA for each $h_M(k)$.

If the distribution of $s(n)$ is sub-Gaussian (such that $(E\{s_R^4(n)\} - 3E^2\{s_R^2(n)\}) < 0$), then all the prespecified \mathbf{h}_M (with the associated I_M) for $M \geq 2$ can be shown to be unstable equilibria (saddle points) by applying the concept proposed by Foschini [7]. Consequently, all the stationary points depicted in Fig. 1 are saddle points when $M \geq 2$.

B. Desired Global Minima and Unstable Equilibria of the MMA When $M = 1$

When $M = 1$ (as in steady-state mode operation) and $\theta(k) \in \{0, \pi/2, \pi, 3\pi/2\}$, (10) yields $h_1(k) = h_{1,R}(k) + jh_{1,I}(k) = 1, j, -1, -j$, which can be shown to be the only four local (hence, global) minima of the MMA, as depicted in Fig. 2, as obtained using (3) with $M = 1$ for a

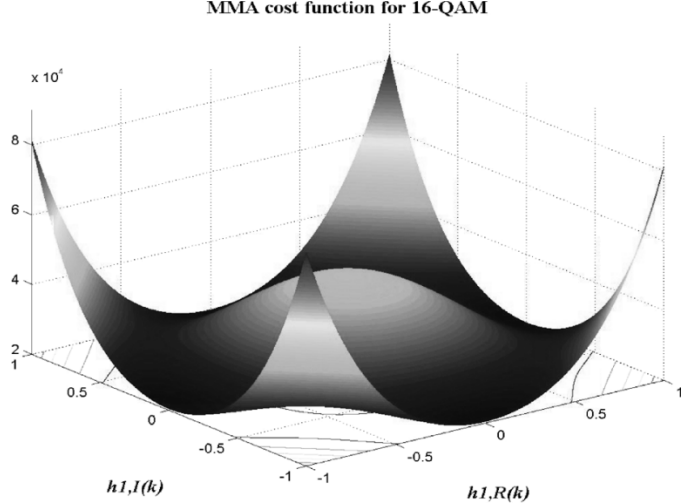


Fig. 2. MMA cost function for a 16-QAM input (for $M = 1$) in terms of $h_{1,R}(k)$ and $h_{1,I}(k)$.

16-QAM input, by using the second derivatives test (as in [8, pp. 768]) for a sub-Gaussian input (such as a QAM channel input). The combined channel-equalizer impulse response of the MMA can be demonstrated to globally converge to the ideal form $\mathbf{h}_1 = [0, 0, \dots, 0, h_1(k), 0, \dots, 0, 0]^T$. This result is in contrast to that of the CMA, whose set of minima is given by $|h_1(k)|^2 = h_{1,R}^2(k) + h_{1,I}^2(k) = 1$ (on the unit circle), which achieves the desired response $y(k) = e^{j\theta(k)}s(k)$, where $-\pi \leq \theta(k) \leq \pi$. Clearly, the CMA cannot correct any phase error. Therefore, the difference between the locations of the minima obtained using CMA and MMA reveals that the former algorithm is phase-blind, while the latter algorithm can compensate for the phase ambiguities, in addition to magnitude equalization.

When $M = 1$ and $\theta(k) \in \{\pi/4, 3\pi/4, 5\pi/4, 7\pi/4\}$, (10) yields the four equilibria

$$h_1(k) = h_{1,R}(k) + jh_{1,I}(k) = \sqrt{\frac{2E\{s_R^4(n)\}}{E\{s_R^4(n)\} + 3E^2\{s_R^2(n)\}}} e^{j\theta(k)}$$

where $\theta(k) = \pi/4, 3\pi/4, 5\pi/4, 7\pi/4$. These equilibria can be shown to be unstable (four saddle points) by using the second derivatives test [8] if the channel input is sub-Gaussian. Fig. 2 displays these four saddle points located at $[h_{1,R}(k), h_{1,I}(k)] = [\pm 0.5945, \pm 0.5945]$ for a 16-QAM input.

C. Phase-Tracking Capability of the MMA

The MMA can be demonstrated to incorporate implicitly a discrete-time, first-order PLL once the algorithm starts functioning. The dynamic phase-tracking feature remains effective during both the transient (startup) and steady-state mode operations of the MMA. Fig. 1 indicates that the phase estimate $\theta(k)$ is partitioned into four parts: $-\pi/4 < \theta(k) < \pi/4$, $\pi/4 < \theta(k) < 3\pi/4$, $3\pi/4 < \theta(k) < 5\pi/4$, and $5\pi/4 < \theta(k) < 7\pi/4$. The part for which $0 < \theta(k) < \pi/4$ is considered first. Since $-E\{s^4(n)\}r^3(k)\sin 4\theta(k) > 0$ for $0 < \theta(k) < \pi/4$, (notably, $E\{s^4(n)\} < 0$ for a QAM

input), the gradient with respect to $\theta(k)$ for a fixed value of $r(k)$, $\nabla_{\theta} J_{\text{MMA}}(n) = -E\{s^4(n)\}r^3(k)\sin 4\theta(k)$ [see (5)], moves counterclockwise. However, the MMA employing the steepest-descent method [i.e., $-\nabla_{\theta} J_{\text{MMA}}(n)$] moves in the opposite (or clockwise) direction. Consequently, the MMA tends to be attracted to the stationary point at $(r_+(M), 0)$ except when $\theta(k) = \pi/4$ exactly [which may occur very rarely in practical implementation of using (1)]. When $\theta(k) = \pi/4$ exactly, $-\nabla_{\theta} J_{\text{MMA}}(n) = 0$, as a result, the MMA will be attracted toward the stationary (saddle) point at $((1/\sqrt{2})r_-(M), (1/\sqrt{2})r_-(M))$. Similarly, the MMA tends to be attracted toward the stationary point at $(r_+(M), 0)$ for $-\pi/4 < \theta(k) < 0$, except when $\theta(k) = -\pi/4$ exactly. When $\theta(k) = -\pi/4$ exactly (in practice, this situation is rare in occurrence), the MMA will be attracted to the stationary (saddle) point at $((1/\sqrt{2})r_-(M), (-1/\sqrt{2})r_-(M))$. For the other three parts, the MMA can be similarly demonstrated to be attracted toward the stationary points at $(0, r_+(M))$, $(-r_+(M), 0)$, and $(0, -r_+(M))$, respectively.

In the special case for which $M = 1$, the MMA tends to converge to the minimum at $[h_{1,R}(k), h_{1,I}(k)] = [1, 0]$ for $0 < \theta(k) < \pi/4$ (Fig. 2). This phase-tracking algorithm essentially performs the function of a discrete-time, first-order PLL described by

$$\begin{aligned}\theta(k+1) &= \theta(k) - \mu \cdot \nabla_{\theta} J_{\text{MMA}}(n) \\ &= \theta(k) - [-\mu \cdot E\{s^4(n)\} \cdot r^3(k)] \sin 4\theta(k) \\ &= \theta(k) - \mu_{\theta}(k) \sin 4[\theta(k) - 0].\end{aligned}$$

(That is, the phase $\theta(k)$ is corrected by an amount proportional to the sine of four times the angular difference between the phase of the equalizer output and the desired phase, which is zero.) Notably, this phase-tracking capability follows naturally from the MMA alone, rather than from an additional carrier-tracking loop. Similarly, for the other three parts, the MMA tends to converge to the three minima, $[h_{1,R}(k), h_{1,I}(k)] = [0, 1]$, $[h_{1,R}(k), h_{1,I}(k)] = [-1, 0]$, and $[h_{1,R}(k), h_{1,I}(k)] = [0, -1]$, respectively. The corresponding phase-tracking algorithms are $\theta(k+1) = \theta(k) - \mu_{\theta}(k) \sin 4[\theta(k) - \pi/2]$, $\theta(k+1) = \theta(k) - \mu_{\theta}(k) \sin 4[\theta(k) - \pi]$, and $\theta(k+1) = \theta(k) - \mu_{\theta}(k) \sin 4[\theta(k) - 3\pi/2]$. Notably, this phase ambiguity in the equalizer output is unavoidable, and it follows from the fact that the QAM input is quadrantly symmetric, so errors that are multiples of 90° in the phase are undetectable. However, differential coding can correct this 90° phase ambiguity.

IV. COMPUTER SIMULATIONS

Suppose that the equalizer input is $u(n) = \sum_{i=0}^{M-1} c(i)s(n-i)e^{j\phi(n)} + w(n)$, where $s(n)$ is an i.i.d. 16-QAM sequence, and $\phi(n) = 2\pi n\Delta f/R$ is a carrier-phase error in which $\Delta f/R = 10^{-4}$ is a carrier frequency offset (CFO) and R is the symbol rate [5]. A complex channel shown in [9] introducing an arbitrary phase rotation is used in the computer simulations. The real and imaginary parts of the complex-valued AWGN $w(n)$ are assumed to be independent, and have equal variance such that the SNR is 30 dB. The simulation experiments described herein employed a complex equalizer with a transversal filter

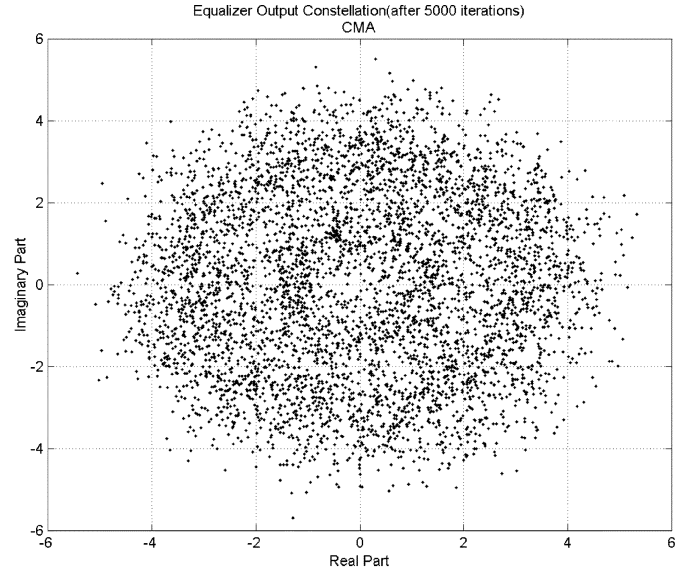


Fig. 3. CMA equalizer output constellation of 16-QAM after 5000 iterations, using a complex channel which introduces an arbitrary phase rotation with an additional CFO $\Delta f/R = 10^{-4}$.

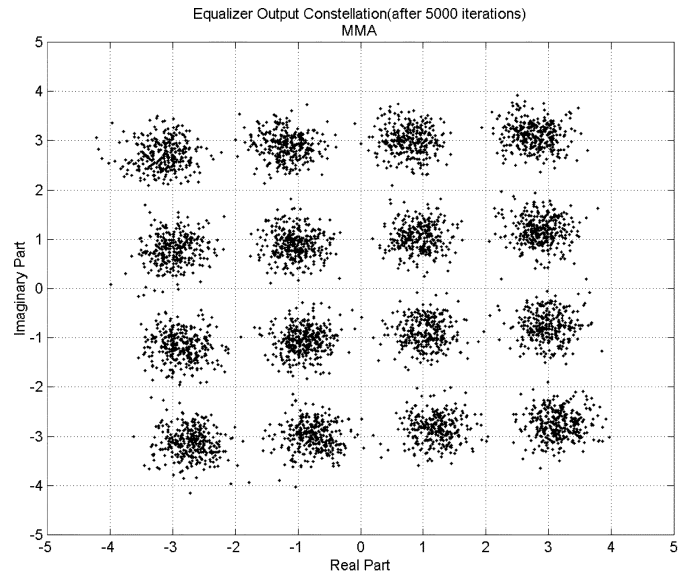


Fig. 4. MMA equalizer output constellation of 16-QAM after 5000 iterations, using a complex channel which introduces an arbitrary phase rotation with an additional CFO $\Delta f/R = 10^{-4}$.

structure having 11 tap weights with five units of time delay. All the tap weights were initialized by setting the central tap weight to 1, and the others to zero. Figs. 3 and 4 depict that both the CMA and MMA are able to achieve magnitude equalization successfully. However, the MMA is capable of recovering the phase rotation caused by the channel, as well as the spinning phase error due to frequency offset, whereas the CMA appears to be spinning due to the CFO.

V. CONCLUSION

This letter has demonstrated that the MMA cost function has only four local (hence, global) minima if $\mathbf{h} = [0, 0, \dots, h_1(k), 0, \dots, 0]^T$ and $h_1(k) = 1, j, -1, -j$. Hence, a gradient search algorithm for minimizing $J_{\text{MMA}}(n)$

is expected to converge to the only four global minima that correspond to the desired response $y(k) = e^{j\theta(k)}s(k)$, where $\theta(k)$ is allowed only to be $0, \pi/2, \pi$, and $3\pi/2$. The key lies in the fact that the cost function of the MMA includes the term $E\{s^4(n)\} \sum_i r^4(i) \cos 4\theta(i)$, which contains the phase information of the blind equalizer output. This phase information enables a possible phase error to be removed. Consequently, the MMA may remove phase jitter without the use of a separate carrier-tracking loop, unlike the CMA, whose cost function is insensitive to the phase of the equalizer output such that the CMA alone cannot achieve phase recovery, causing an additional carrier-recovery system (such as a PLL) to be required for phase recovery. Therefore, the MMA may solve a possible phase-ambiguity problem inherent in the CMA. However, the existence of this term may appear to result in one potential disadvantage of the MMA, because four additional saddle points at $(\pm(1/\sqrt{2})r_-(M), \pm(1/\sqrt{2})r_-(M))$ are generated in (5). As a result, the MMA, using the stochastic gradient-descent method, may be first attracted toward the vicinity of one of the saddle points, around which it exhibits slow convergence, before converging to the desired minimum.

REFERENCES

- [1] D. N. Godard, "Self-recovering equalization and carrier tracking in two-dimensional data communication system," *IEEE Trans. Commun.*, vol. COM-28, no. 11, pp. 1867–1875, Nov. 1980.
- [2] J. R. Treichler and M. G. Larimore, "New processing techniques based on the constant modulus algorithm," *IEEE Trans. Acoust., Speech, Signal Process.*, vol. ASSP-33, no. 4, pp. 420–431, Apr. 1985.
- [3] C. R. Johnson *et al.*, "Blind equalization using the constant modulus criterion: A review," *Proc. IEEE*, vol. 86, no. 10, pp. 1927–1950, Oct. 1998.
- [4] Y. Li and Z. Ding, "Global convergence of fractionally spaced Godard (CMA) adaptive equalizers," *IEEE Trans. Signal Process.*, vol. 44, no. 4, pp. 818–826, Apr. 1996.
- [5] K. N. Oh and Y. O. Chin, "Modified constant modulus algorithm: Blind equalization and carrier phase recovery algorithm," in *Proc. IEEE Int. Conf. Commun.*, vol. 1, 1995, pp. 498–502.
- [6] J. Yang, J.-J. Werner, and G. A. Dumont, "The multimodulus blind equalization and its generalized algorithms," *IEEE J. Sel. Areas Commun.*, vol. 20, no. 6, pp. 997–1015, Jun. 2002.
- [7] G. J. Foschini, "Equalization without altering or detecting data," *AT&T Tech. J.*, vol. 64, pp. 1885–1911, Oct. 1985.
- [8] J. Stewart, *Calculus*, 2nd ed. Pacific Grove, CA: Brooks/Cole, 1991.
- [9] D. Hatzinakos, "Blind equalization using stop-and-go adaptation rules," *Opt. Eng.*, vol. 31, no. 6, pp. 1181–1188, Jun. 1992.